Mobility of Surfactants in and between Adsorbed Monolayers

A. D. Berman,[†] S. D. Cameron,[‡] and J. N. Israelachvili*,[†]

Department of Chemical Engineering, University of California, Santa Barbara, California 93106, and Exxon Research and Engineering, Route 22 E, Clinton Township, Annandale, New Jersey 08801

Received: January 16, 1997; In Final Form: April 14, 1997[⊗]

Using X-ray photoelectron spectroscopy (XPS), the lateral interdiffusion of ionic surfactants in adsorbed monolayers and their exchange between two contacting monolayers were measured under varying conditions of temperature and humidity. Measured interdiffusion coefficients at 25 °C were of order $(1-10) \times 10^{-9}$ cm^2/s, and exchange half-times were of order 1 h (even longer for totally dry conditions). These low diffusion and exchange rates result from the complex rate-limiting interdependence of different migrating surfactant molecules and their counterions. The rate-limiting factors to both diffusion and exchange were found to be (1) steric constraints, i.e., the need to conserve the packing density or average molecular area when molecules move or exchange positions, (2) electroneutrality constraints, i.e., the need to maintain local electroneutrality at all places at all times, (3) confinement constraints in trapped monolayers, i.e., mild (low pressure) compressive confinement seems to have only a small effect on diffusion rates, and (4) temperature and humidity, i.e., higher temperatures and humidity generally increase both the diffusion and exchange rates.

Introduction

Surfactant monolayer coatings are often important features of colloidal systems and play a pivotal role in lubrication systems. Nonaqueous colloidal systems often fail due to aggregation of the particles because of the strong, short-ranged van der Waals forces. However, surfactant coatings can keep the particles dispersed through steric stabilization.[1,2] It has also been demonstrated that monolayer coatings can be effective boundary lubricant films, reducing friction and protecting sliding surfaces from wear.[3,4] While the equilibrium (static) properties of adsorbed surfactant monolayers have been much studied, they do not provide a complete picture for understanding colloidal and lubrication systems under nonequilibrium (dynamic) conditions, for example, during mixing, sliding, or flow. Through the processes of diffusion, surface collisions, and shearing, adsorbed surfactant molecules can exchange between different surfaces (either through direct contact or via the solvent) and rearrange laterally or flip-flop on the same surface. Exchange between contacting monolayers and lateral diffusion along a surface are the primary mechanisms for surfactant redistribution in colloidal systems, and these are the two processes investigated in this paper.

The mobility of lipids in free bilayers in aqueous environments has been studied extensively, giving flip-flop and exchange rates of $10^{-3}-10^{-1}$ h^{-1} and lateral diffusivities of $10^{-8}-10^{-6}$ cm^2/s.[5−8] Lateral diffusion studies of surfactants in monolayers at an air−water interface give similar values,[9,10] while diffusivities of amphiphiles in the outer layer of a supported bilayer were measured to be slightly lower—on the order of $10^{-8}-10^{-7}$ cm^2/s.[11] However, the outer monolayers of bilayers (supported or free) are expected to be inherently different from adsorbed monolayers where the direct interaction between the solid substrate and the surfactant polar heads can radically change the ordering and mobility.

Early studies by Rideal and Tayadon[12,13] investigated the transfer of radio-labeled stearic acid from a monolayer surface to a bare surface pressed into contact with the monolayer. They found, as expected, that for identical substrates the surfactant eventually partitioned itself equally between the two surfaces and that the rate of transfer increased with increasing temperature and relative humidity. Surface diffusion was measured for a single-component monolayer, and activation energies for the diffusion process were calculated. Gaines, in a series of papers,[14,15] further analyzed the results of Rideal and Tayadon[12,13] and corrected the transfer rates between the surfaces. This work also showed that the transfer between two monolayer-coated surfaces (compared to the transfer between a monolayer and a bare surface) proceeded at a substantially slower rate. More recent work by Neuman et al.[16] discussed the lateral diffusivity of surfactants under confinement between two molecularly rough surfaces. This was done by measuring fluorescence recovery after photobleaching (FRAP) of a dilute fluorescent probe embedded in the adsorbed monolayers and assuming that the tracer had dynamics similar to the surrounding surfactant molecules.

The different types of surfactant migration are illustrated in Figures 1A and 2A. They include transfer, exchange, flip-flop, and lateral diffusion. Transfer and exchange involve movement of a surfactant molecule between two different surfaces, while flip-flop and lateral diffusion refer to the migration of a surfactant molecule across or along *one* monolayer surface; lateral diffusion of a free monolayer can be contrasted to diffusion under confinement. In particular, the migrating species include the amphiphilic molecules and their counterions. Thus, to obtain a complete picture, all species involved in the transport must be considered together since their motions are generally coupled.

This work examines the mobilities of more complex surfactants adsorbed as monolayers on a solid substrate, using electron spectroscopy for chemical analysis (ESCA) to directly measure the changing surface concentrations of the migrating amphiphiles and their counterions: the exchange rates of surfactants and counterions between two contacting monolayer coated surfaces were measured, as well as the binary lateral diffusion of different surfactants along a single surface. In addition, the effects of confinement on lateral diffusion were examined. Focus was placed on the effects of temperature and humidity on migration

* To whom correspondence should be addressed.
[†] University of California, Santa Barbara.
[‡] Exxon Research and Engineering.
[⊗] Abstract published in *Advance ACS Abstracts,* July 1, 1997.

S1089-5647(97)00238-1 CCC: $14.00

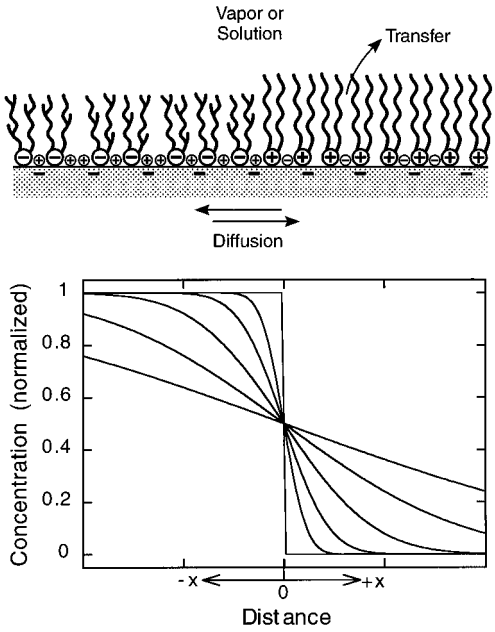

Figure 1. (A, top) Schematic diagram of the initial arrangement of surfactants and counterions on the mica substrate for lateral diffusion measurements. The adsorbed species diffuse along their concentration gradients in a coordinated fashion to maintain charge neutrality at each point along the surface. (B, bottom) Theoretical concentration profiles from eq 2 for different diffusion times.

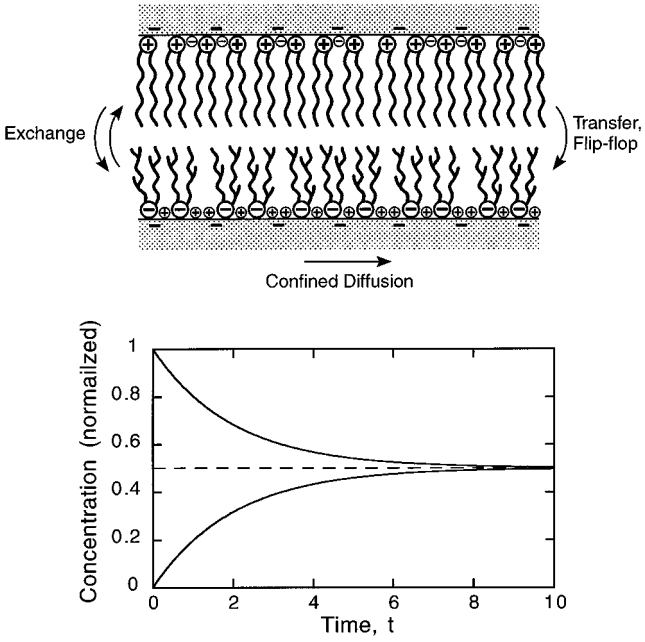

Figure 2. (A, top) Schematic of the exchange experiments where dissimilar monolayer surfaces are contacted for varying amounts of time The mechanisms involved are transfer, exchange, and flip-flop of the surface species. (B, bottom) Concentration of the migrating species on each of the surfaces as a function of time in contact, according to eq 3.

dynamics. The data indicate a strong coupling of the migration of all the charged species to ensure that local charge neutrality is maintained at all times.

Theoretical Background

Adsorbed species may be considered to migrate along a surface through a series of jumps between adjacent lattice sites. On a continuum level this process can be described as a diffusional process with an activity gradient as the driving force. In these terms, migration of surfactants along a surface or between two surfaces can be described by the diffusion equation[17]

$$\partial c/\partial t = D\nabla^2 c \tag{1}$$

where c is the concentration of the surface species, t is the time, and D is the surface diffusivity.

The experiments described here aim to measure the surface diffusivities of amphiphiles and their counterions. To measure the diffusivity, a concentration gradient is established on a single surface, as illustrated in Figure 1A, and the concentrations of surface species are then measured as a function of position and time. For the step concentration profile at $t = 0$ illustrated in Figure 1A,B, the solution to eq 1 is

$$\frac{c(x,t)}{c_\infty} = \frac{1}{2}\left[1 \pm \mathrm{erf}\left(\frac{|x|}{2\sqrt{Dt}}\right)\right] \tag{2}$$

where c_∞ is the concentration far from the interface, x is the diffusion direction distance, erf(z) is the error function, and the $\pm$ depends on the direction of diffusion. Theoretical concentration profiles $c(x)$ according to eq 2 are plotted for different diffusion times in Figure 1B.

For exchange between two opposing surfaces (Figure 2A), the kinetics can be described as a partitioning of surfactant species between two phases corresponding to the two monolayers. For the case of surfactant transferring from a monolayer-coated surface to another surface (Figure 2A), the concentration on each surface decays exponentially (ideally to an equal distribution on both surfaces) according to the equation

$$c(t) = (c_0/2)(1 \pm e^{-t/\tau}) \tag{3}$$

where c_0 is the initial concentration on the monolayer surface, τ is the characteristic exchange time, and the $\pm$ depends on the migration direction. A theoretical time profile of the concentrations for two contacting surfaces is illustrated in Figure 2B.

Experimental Section

Materials. The selection of surfactants for this study was based on general interest and on practical considerations such as compatibility with the ESCA technique used for the elemental analysis. A double-chained cationic surfactant dihexadecyldimethylammonium chloride (DHDACl) was obtained from Sogo Pharmaceutical Co., LTD, Japan, as the bromide salt. The bromide was ion-exchanged with chloride as previously described.[18] An anionic calcium alkylbenzenesulfonate (CaABS) surfactant was obtained from Exxon Chemical Co. (Annandale, NJ). This surfactant has a saturated randomly branched C_{24} (average) hydrocarbon tail with an anionic benzenesulfonate headgroup. The alkyl tail is attached to the phenyl ring at a random point, and calcium is the counterion of the surfactant. The CaABS was purified as previously described.[19] These surfactants were selected for the diffusion studies because of their technological use, because of the morphology of the monolayers they form, and because they each have a distinct headgroup and counterion that is detectable, quantifiable, and distinguishable when probed with ESCA.

Surface Preparation. For both the diffusion and exchange studies, surfactant monolayers were deposited on freshly cleaved, molecularly smooth mica substrates. For the lateral diffusion experiments the samples were ~3 × 10 cm, while exchange-only experiments used smaller samples (~3 × 3 cm).

Langmuir−Blodgett (LB) deposition was used to make monolayers with a controlled starting surface density. For

homogeneous monolayers (single-surfactant coatings), the surfactant was spread on an air−water interface and then compressed to the desired surface pressure. The mica substrate was then lifted slowly through the air−water interface, resulting in a monolayer with known surface coverage.

Adjacent monolayers on a single mica surface used for lateral diffusion measurements (Figure 1A) were prepared in a modified LB manner as follows: initially, the deposition proceeds as with the conventional LB technique. When the substrate is halfway through the air−water interface, the deposition is stopped, and the air−water interface is aspirated clean to remove the surfactant from the water surface. The second surfactant is then spread on the air−water interface and compressed to the desired surface pressure. During this process the three-phase, mica−water−air contact line remained "pinned" at the same place on the mica surface, and the meniscus "contact" angle (which was small on the water side) did not change; this favorable condition arises, in part, because during aspiration the water level does not appreciably change due to the large volume and surface area of the trough. The deposition of the second surfactant then proceeds by continuing to pull the substrate through the air−water interface as before. The sharpness of the boundary between the adjacent monolayers was better than 0.5 mm as ascertained from subsequent wettability tests where a droplet of water, placed across the interface, becomes asymmetrical, adopting a D-shape, where the width of the straight boundary defines the width of the boundary dividing the two monolayers. We note that the sharpness of the interface ($<$0.5 mm) is smaller than the distances (0.5−2.0 mm) between sampling points in the ESCA measurements and about an order of magnitude smaller than the width of the transition region (shown later in Figure 3).

The monolayer depositions of CaABS and DHDACl were done at a surface pressure of $\prod = 28$ mN/m, resulting in surface coverages of 65 and 71 Å^2/molecule, respectively.[20] Previous SFA and dynamic contact angle measurements of the adhesion and contact angle hysteresis,[21] friction forces,[22] elastic compressibility,[20] and self-assembly[23,24] of DHDACl, CaABS, and other monolayers on mica have indicated the conditions under which they may be considered to be in the frozen (or solidlike) state, the amorphous state, or the liquid (or fluidlike) state. These measurements indicate that at these surface coverages the chains in the monolayers are in the amorphous or fluidlike state.

Due to the ionic character of mica surfaces, which has exchangeable K^+ counterions, the deposition of DHDACl resulted in an ion exchange of $DHDA^+$ for K^+, with no detectable Cl^- adsorbing to the surface. Similarly, the ABS^- was deposited at a constant surface pressure, where the excess Ca^{2+} cations exchanged with the mica K^+, resulting in a Ca^{2+}-rich surface (i.e., more Ca than in the stoichiometric formula $Ca(ABS)_2$).

For interdiffusion experiments on a single biphasic monolayer at different humidities, the surfaces were placed in the appropriate temperature- and humidity-controlled atmosphere immediately after the deposition. For the exchange experiments at different humidities, each monolayer was first equilibrated with humid atmosphere at the desired RH for 2 days. The two monolayers were then brought into contact and placed in a temperature and humidity controlled chamber. For the confined diffusion experiments, the two monolayers were brought into contact immediately after the depositions.

True molecular contact was established by laying one surface down over the other, starting at one edge, and applying a slight pressure with a "rolling pin" action. If the surfaces were dust-free, they spontaneously came into contact at one point which suddenly became darker; this was followed immediately by the spreading of the darkened region over the whole area (typically $\sim$10 cm^2). After this, the surfaces were stuck together and could not be pulled away without applying a pulling or peeling force. This procedure established that the surfaces were in self-adhesive contact. Samples showing poor or incomplete contact over the whole area were not used.

Surface Analysis. The concentration profiles of the surfactants and their counterions were measured using ESCA. The ESCA system was a Physical Electronic Model 5600 with a hemispherical analyzer and modified with a small area lens. The X-ray source was an Al anode Kα at 1486.6 eV run at 300 W. This technique allows for the quantification of elemental species on the surface of materials. Local surface concentrations were measured with a lateral resolution of 1 mm with a measurement spot size of 1 mm. Due to the low kinetic energy of the emitted photoelectrons, only those emitted close to the surface are not scattered or reabsorbed. Therefore, ESCA detects elemental species only within $\sim$50 Å of the surface, making it highly sensitive to species present in monolayers. Measurement of surface concentrations by ESCA is a nondestructive, reproducible process. The energy supplied to the monolayer species by the absorption of soft X-rays is released in the kinetic energy of the photoemitted electrons and X-ray fluorescence photons with only a small amount transferred to vibrational modes. The greatest effect on the sample comes from the thermal electrons produced from the Al foil screening the sample from the ionization source. To minimize this effect, the distance between the source and the sample was optimized to produce no change in the surface coverage of the surfactant over the period of the experiments while maintaining reasonable collection times.

The selection of surfactants to study was based partially on their suitability for study by ESCA. DHDACl was studied by measuring the N in the surfactant and Cl as the counterion. Similarly, CaABS has S in the surfactant and Ca as the counterion. Each of these four elements has a unique ESCA signal that is distinguishable from the other and from the mica substrate (which also contributes to the measured signal). The spectra were collected at 71 eV pass energy with 0.10 eV steps. High-energy resolution was not required because only surface concentrations were measured. All spectra were all collected at a 45° take-off angle to provide an appropriate probe depth and to maintain consistency from sample to sample.

While ESCA can be used for absolute quantification of surfactant concentrations on a surface,[25] this experiment was concerned with relative changes in quantities of the various mobile species. Concentrations of the surfactants and counterions were normalized by the measured Si concentration, which has a strong reference signal from the mica substrate. Relative surface concentrations were measured this way and were used in calculating mobilities of the adsorbed species.

Results

Lateral Diffusion. Lateral concentration profiles of adjacent monolayers (Figure 1A) were measured after a certain diffusion time under fixed environmental conditions. Diffusivities of the various species were calculated by fitting the concentration profiles to eq 2 (Figure 1B). Characteristic surface concentration profiles at $t = 5.4 \times 10^5$ s ($\sim$6 days) and the fits from eq 2 are illustrated in Figure 3A. Salient features, which are described in greater detail below, are (1) the excluded areas of the surfactant molecules (steric effects) modulate the relative diffusivities of the different surfactants (i.e., when two different species having different molecular areas interdiffuse, they do

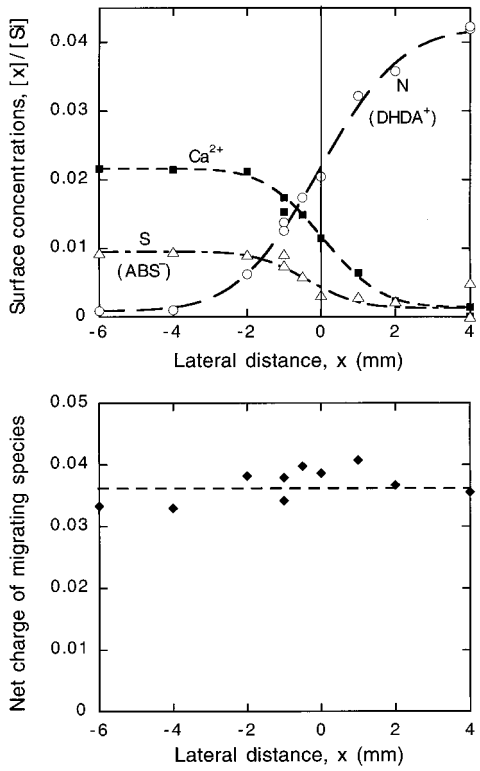

Figure 3. Lateral diffusion: (A) Concentration profiles for the mobile ionic species $DHDA^+$, ABS^-, and Ca^{2+} for a free diffusion experiment within a single, initially biphasic, monolayer of $DHDA^+Cl^-$ and $Ca^{2+}ABS^-$ at $T = 25$ °C and 100% RH at time $t = 5.4 \times 10^5$ s. The data are fit by the theoretical curves from eq 2 with the diffusivity, D, as the adjustable parameter. (B) Net charge of the mobile species, $[DHDA^+] - [ABS^-] + 2[Ca^{2+}]$, was summed and plotted as a function of position along the diffusion surface. The relatively constant value over the surface is *further* evidence that charge neutrality conservation plays an important role in the migration of ionic species.

TABLE 1: Lateral Diffusion of Surfactants and Counterions along the Mica Substrate

			$D \times 10^8$ (cm²/s)		
type	RH (%)	T (°C)	$DHDA^+$	ABS^-	Ca^{2+}
free diffusion	55	25	1.1	0.9	0.55
(single monolayer)	100	25	2.8	1.1	1.5
	55	100	8.4	1.2	3.8
confined diffusion	55	25	0.8	0.7	0.37
	100	25	17	14	9.9

so while conserving their coverage density which is different from a one-to-one *molecular* exchange, (2) diffusion is strongly charge-coupled (Figure 3B), i.e., different ionic species migrate while maintaining overall local charge neutrality at all places at all times, and (3) increasing the temperature and water vapor pressure (humidity) substantially facilitates diffusion. Thus, in these experimental results one can observe the competing and complementary effects of activity gradients (concentration and electrostatic potential gradients) driving diffusion *vs* steric barriers and diffusion jump activation energies impeding the diffusion rate. The lateral diffusivities of the various amphiphilic and ionic surface species under different conditions are listed in Table 1.

Steric Effects. Through the various experiments under different conditions the $DHDA^+$ surfactant had a higher diffusivity than ABS^-, which is due primarily to steric effects. Because of the high packing density of the $DHDA^+$ surfactant, ABS^-, with its bulky hydrocarbon chains, was sterically hindered from rapidly diffusing into the $DHDA^+$-rich side of the substrate. In contrast, the relatively low hydrocarbon chain packing density of the ABS^- surfactant allowed for the $DHDA^+$ amphiphiles to diffuse more easily. These are reflected in the slightly higher diffusivities observed for $DHDA^+$.

Dynamic contact angle measurements (which by virtue of the long surfactant relaxation times may not be the equilibrium or static values[21]) were made to qualitatively confirm the relative hydrophobicities and chain packing densities of the DHDACl and CaABS monolayers. Advancing water contact angles, which probe the native states of the monolayers,[21] showed very different hydrophobicities of the two monolayer surfaces: DHDACl had an advancing angle of 104°, compared to 26° on the CaABS monolayer. The dramatic difference in hydrophobicity is partially due to the closer packing of the hydrocarbon chains of DHDACl.

Electrostatic Effects. While steric effects tend to govern the intrinsic diffusivities of the surfactants, electrostatic interactions further regulate the relative mobilities of the various adsorbed ionic species. Instead of the surfactants diffusing strictly with their counterions, they tended to diffuse independently or with "foreign" counterions, but with the restriction of local charge neutrality being obeyed which controlled the relative migration rates of the various charged species. Figure 3B shows the net charge of the diffusing species at each point along the surface at time $t = 5.4 \times 10^5$ s. (The concentrations of the individual species are shown in Figure 3A.) Because of the relatively high concentration gradient of calcium and its small steric diffusion barrier, Ca^{2+} was the driving force for diffusion. Due to the Donnan effect,[26] the flux of Ca^{2+} was countered by the diffusion of $DHDA^+$ in the opposite direction to maintain charge neutrality. Codiffusion of ABS^- with the calcium cations also occurred, but was less of a factor in maintaining charge neutrality because of the relatively low initial concentration of the benzenesulfonate surfactant.

Diffusion under Confinement. Lateral diffusion rates under confinement were measured by contacting a surface having a biphasic monolayer (Figure 1A) with a homogeneous (single component) monolayer. Because exchange between the two contacting monolayers is much quicker than lateral diffusion over the millimeter length scales measured, the surfaces quickly reached local *exchange* equilibrium (as described below) and then tended toward lateral diffusion equilibrium. The concentrations of the mobile species at each point along one surface were essentially identical to the concentrations at the corresponding point on the other contacting surface, so a single value for D was calculated for each of the species from the two contacting surfaces. The measured values for D were not appreciably different from unconfined, single-surface diffusion at 25 °C, 55% relative humidity (RH) (about 25%—much less than the order of magnitude changes brought about by changing the temperature and humidity). This shows that the largest hindrances to diffusion are the headgroup/substrate and hydrocarbon tail/tail interactions, which are not appreciably affected by confinement.

Effect of Humidity. Humidity is known to play an important role in the migration and other properties of charged species on mica and other ionic surfaces.[27,28] Because of the strong ionic interactions between mica and the adsorbed species, there is a relatively high activation barrier for species to desorb from one lattice site to jump to the next. Under conditions of high humidity, water penetrates into the headgroup regions[19,24,27,28] and weakens the ionic bonds; this results in a weaker headgroup−substrate interaction and thus a smaller activation barrier for diffusion. The result, as shown in Table 1, is that unconfined diffusion at 100% RH (saturation) is ~2.5 times faster than at 55% RH. In the case of confined diffusion, the effective

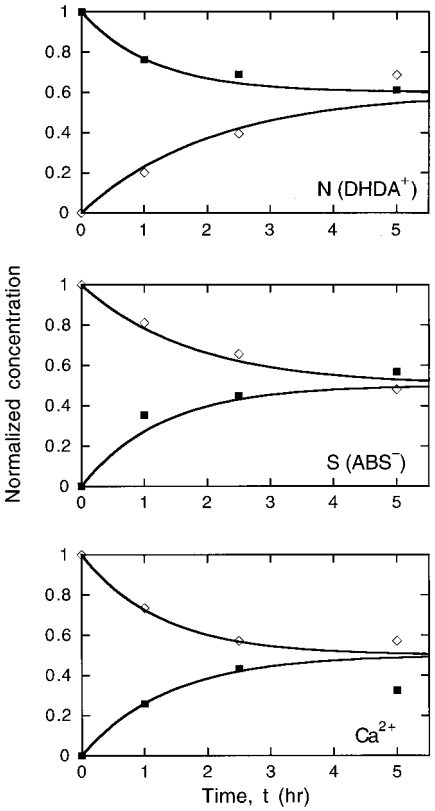

Figure 4. Exchange kinetics: The concentration of the mobile species on each of the contacting surfaces is plotted as a function of time in contact at $T = 25$ °C, 100% RH. Solid lines are the fits to eq 3 for each of the measured species where the characteristic exchange times and asymptotic concentrations were free parameters (i.e., a final concentration of 50/50 was not assumed a priori). In parts B and C the values do go toward 50/50, as expected, but in (A) they appear not to. This is almost certainly due to measuring errors.

TABLE 2: Surfactant and Counterion Exchange between Two Contacting Monolayer Surfaces

		time, τ (h)			rate, k (h^{-1})		
RH (%)	T (°C)	$DHDA^+$	ABS^-	Ca^{2+}	$DHDA^+$	ABS^-	Ca^{2+}
100	25	1.6	1.5	1.3	0.31	0.33	0.38
100	100	0.15	0.10	0.24	3.3	5.0	2.1

diffusivity increases by ~32 times for the same humidity change. This is because bulk water can condense (capillary condensation) between the surfaces, thereby further fluidizing and changing the morphology of the contacting monolayers.[21,27,28]

Exchange. Experiments measuring the exchange of surfactants and counterions between two contacting monolayers demonstrated trends similar to those observed in the lateral diffusion measurements. Contacting monolayer surfaces were separated after fixed times in contact, and the surface concentrations as a function of contact time were fitted to eq 3 to determine the exchange time constant τ. This can be related to an exchange rate constant, $k = (2\tau)^{-1}$, assuming a unimolecular process. A characteristic data set is illustrated in Figure 4, along with the corresponding fits to eq 3. As in the case of lateral diffusion, the transfer rates of $DHDA^+$ and ABS^- were comparable. Table 2 lists the τ values for exchange of the different species and the associated exchange rate constants k. Although the activation barrier for exchange is expected to be higher than for lateral diffusion because the ionic surfactant headgroup must migrate through the hydrophobic tails section, the time scales for exchange are much shorter than for lateral migration experiments. The reason for this is that the distance scale in exchange is <10 nm, which is substantially shorter than the ~10 mm lateral diffusion lengths. To compare the rates of exchange with lateral diffusion in a more meaningful way, calculations were made for the lateral diffusion time required for the concentration at $x = 10$ nm to fall to 1/e of the equilibrium value. Using the measured lateral diffusivity of $D = 3 \times 10^{-8}$ cm^2/s, the calculated time is 2×10^{-8} h, or roughly 10^8 times *faster* than exchange over the same distance.

Measuring Errors. Since only one sample was probed at each condition (of humidity, temperature, confinement, etc.), the systematic errors in the data points shown cannot be established unambiguously. However, the trends in the results from one position to another, from one time to another, and between confined and unconfined monolayers are all consistent with errors that are less than 10% for each data point shown in Figures 3 and 4.

Temperature Effects. Lateral diffusion and exchange rates were measured at 25 and 100 °C to get an idea of the magnitude of the activation energies for the different migration processes at 55% RH. Over this temperature range the lateral diffusivities increase by a factor of 6, while the exchange rates increased 15 times. The Arrhenius law can be used to relate rates with the activation energy E_a and T:

$$D = D_0 e^{-E_a/k_B T} \tag{4}$$

The rate increase of the lateral diffusion process corresponds to $E_{a(diffusion)} \approx 5.3$ kcal/mol ($9k_BT$), while the exchange activation energy is $E_{a(exchange)} \approx 7.9$ kcal/mol ($13k_BT$). The diffusion activation energy can be compared to 21 kcal/mol calculated by Rideal and Tayadon.[13] This difference is attributable to the different surfactants used in the different studies and the possibly lower (but unrecorded) humidity in the earlier experiments.

Discussion and Conclusion

The overall transport properties of surfactants are essential for calculating aging times of colloidal suspensions and determining mixing rates for processes and applications. The individual factors that control the transport properties outlined above can thus be used to control colloidal system behavior. For example, trace amounts of water (or other polar components) substantially increase the surfactant mobility and would aid in accelerating redistribution of surfactants through the system. Similarly, elevated temperature would have the same effect by increasing the migration rates. In addition, higher temperatures can further increase surfactant mobility by increasing the water concentration in the colloidal system because of increased solubility of water in the nonpolar phase. However, increasing temperature could also have the opposite effect in a closed system with no reservoir of water by causing the finite water present in the system to partition away from the interfaces and into the solvent because of the increased solubility.

Beyond control of conditions such as temperature and water concentration, the monolayers themselves can be engineered to take advantage of the effects of the physical and chemical contributions to surfactant mobility. The hydrocarbon chain morphology can be selected to determine the optimum packing state and mobility of the surfactant on the surface. Similarly, the headgroup type (ionic, nonionic, zwitterionic) will substantially affect how the surfactant will migrate, especially in the context of the overall system.

These key factors that control the mobility of adsorbed surfactants can be used to achieve a whole range of dynamic behaviors of surface coatings to optimize features ranging from colloidal stability to lubrication performance. In lubrication

systems the surfactant coatings are effective in minimizing the wear rate of rubbing surfaces only when they remain intact and do not expose the underlying substrate. Different surfactant mobilities will therefore determine how easily or quickly a layer comes off or becomes replenished, thereby determining its effectiveness as a wear inhibitor.

In summary, the diffusivities of ionic surfactants and counterions were found to be strongly interdependent and were controlled by three principal factors: Excluded area (steric) effects hinder the diffusion of the amphiphiles along the surface and result in slower migrations of bulkier molecules. Electrostatic effects play an important role in coupling the diffusion rates of charged species to maintain charge neutrality at each point along the surfaces. Changes in mobilities with relative humidity demonstrate the important role of surfactant−substrate interactions in the surface transport properties. In the design of surfactant monolayer coatings for dynamic systems such as lube oils, these factors must be considered to ensure that the desired surface and colloidal properties are maintained during dynamic processes.

Acknowledgment. This work was supported by Exxon Research & Engineering Co., Exxon Chemical Co. (Paramins), and the Department of Energy under Grant DE-FG03-87ER45331. The authors thank Drs. S. Steinberg and R. S. Polizzotti for helpful discussions.

References and Notes

(1) Israelachvili, J. N. *Intermolecular and Surface Forces*, 2nd ed., Academic Press: San Diego, CA, 1991.
(2) Prost, J.; Rondelez, F. *Nature* **1991**, *350*, 11.
(3) Briscoe, B. J.; Evans, D. C. B. *Proc. R. Soc. London* A **1982**, *380*, 389.
(4) Allen, C. M.; Drauglis, E. *Wear* **1969**, *14*, 363.
(5) Marsh, D. *CRC Handbook of Lipid Bilayers;* CRC Press: Boca Raton, FL, 1990; p 203.
(6) Tocanne, J.-F.; Dupou-Cézanne, L.; Lopez, A.; Tournier, J.-F. *FEBS Lett.* **1989**, *257*, 10.
(7) Vaz, W. L. C.; Almeida, P. F. *Biophys. J.* **1991**, *60*, 1553.
(8) Lindblom, G.; Orädd, G. *Prog. NMR Spectrosc.* **1994**, *26*, 483.
(9) Caruso, F.; Grieser, F.; Murphy, A.; Thistlewaite, P.; Urquhart, R.; Almgren, M.; Wistus, E. *J. Am. Chem. Soc.* **1991**, *113*, 4838.
(10) Caruso, F.; Grieser, F.; Thistlewaite, P.; Almgren, M. *Biophys. J.* **1993**, *65*, 2493.
(11) Charych, D. H.; Goss, C. A.; Landau, E. M.; Majda, M. *Mol. Cryst. Liq. Cryst.* **1990**, *190*, 95.
(12) Rideal, E.; Tadayon, J. *Proc. R. Soc. London A* **1954**, *255*, 346.
(13) Rideal, E.; Tadayon, J. *Proc. R. Soc. London A* **1954**, *255*, 357.
(14) Gaines, G. L. *Nature* **1960**, *186*, 384.
(15) Gaines, G. L. *Nature* **1959**, *183*, 1109. Gaines, G. L. *Nature* **1959**, *183*, 1111.
(16) Neumann, R. D.; Park, S.; Shah, P. *J. Phys. Chem.* **1994**, *98*, 12474.
(17) Bird, R. B.; Stewart, W. E.; Lightfoot, E. N. *Transport Phenomena*; Wiley: New York, 1960.
(18) Pashley, R. M.; McGuiggan, P. M.; Ninham, B. W. *J. Phys. Chem.* **1986**, *90*, 5481.
(19) Gee, M. L.; Israelachvili, J. N. *J. Chem. Soc., Faraday Trans.* **1990**, *86*, 4049.
(20) Chen, Y. L.; Helm, C. A.; Israelachvili, J. N. *Langmuir* **1991**, *7*, 2694.
(21) Chen, Y. L.; Helm, C. A.; Israelachvili, J. N. *J. Phys. Chem* **1991**, *95*, 10736.
(22) Yoshizawa, H.; Chen, Y. L.; Israelachvili, J. *J. Phys. Chem.* **1993**, *97*, 4128.
(23) Chen, Y. L.; Chen, S.; Frank, C.; Israelachvili, J. N. *J. Colloid Interface Sci.* **1992**, *153*, 244.
(24) Chen, Y. L.; Xu, Z.; Israelachvili, J. *Langmuir* **1992**, *8*, 2966.
(25) Herder, P. C.; Claesson, P. M.; Herder, C. E. *J. Colloid Interface Sci.* **1987**, *119*, 155.
(26) Eisenberg, D.; Crothers, D. *Physical Chemistry with Applications to the Life Sciences*; Benjamin/Cummings Publishing Co.: Menlo Park, CA, 1979.
(27) Chen, Y. L. E.; Gee, M. L.; Helm, C. A.; Israelachvili, J. N.; McGuiggan, P. M. *J. Phys. Chem.* **1989**, *93*, 7057.
(28) Chen, Y. L.; Israelachvili, J. N. *J. Phys. Chem.* **1992**, *96*, 7752.